SI Appendix

Decorin suppresses tumor lymphangiogenesis: A mechanism to curtail cancer progression

Dipon K. Mondal[1], Christopher Xie[1], Gabriel J. Pascal, Simone Buraschi and Renato V. Iozzo[2]

Department of Pathology and Genomic Medicine, and the Translational Cellular Oncology Program, Sidney Kimmel Cancer Center, Sidney Kimmel Medical College at Thomas Jefferson University, Philadelphia, PA 19107, USA

Materials and Methods

Animals and Cells

6-8 weeks old C57BL/6 mice were purchased from Jackson Laboratories (Bar Harbor, ME) and housed at Thomas Jefferson University (TJU) animal research facility in sterilized filter top cages under 12-h light-dark cycle, humidity, and temperature-controlled conditions. All animal procedures were approved by the Animal Care and Use Committee of TJU. E0771 cells were obtained from ATCC and were maintained in DMEM (Gibco, Thermo Fisher Scientific, Inc.) with 10% FBS (Gibco, Thermo Fisher Scientific, Inc.) and 1% penicillin-streptomycin (Corning, 30-002-CI). Mouse and human primary dermal lymphatic endothelial cells (LECs) were purchased from Cell biologics, used between passages 3 to 6, and were maintained in complete endothelial cell medium (Cell biologics, M1168 and H1168). 0.25% trypsin-EDTA was used to detach and re-culture cells to the next passage. Once the cells reached 70-80% confluency, single or combination treatments were performed according to the experimental need.

Orthotopic E0771 Injection in Mice, Tumor Measurement and Processing

All animals were bred in-house and maintained in specific pathogen-free conditions at Thomas Jefferson University, Jefferson Alumni Hall. All the animal experiments were conducted in accordance with the animal protocol approved by Institutional Animal Care and Use Committee (IACUC) of Thomas Jefferson University. We generated orthotopic breast carcinoma allografts using E0771, triple-negative breast cancer cells derived from C57BL/6 mice (1-5). These cells have a propensity for spontaneous lung (6) and bone (7) metastases, desmoplasia (8) and are syngeneic to our *Dcn*$^{-/-}$ mice (9), which we backcrossed into the C57BL/6 background for >12 passages. To develop tumors in the breast, 1x 10^6 E0771 cells/100 µl were orthotopically implanted into the right fat pad of the fourth mammary gland using a sterile 22-gauge needle. Before injecting the E0771 cells in mice, live cell number was counted with a hemocytometer using 0.4% trypan blue solution (Corning, 25-900-CI). Throughout the study, health status of the mice was checked every 2 days. After Day 10 post-injection when manual palpation revealed existence of a mammary tumor around the injection site, mice were randomly divided into different treatment groups. Recombinant decorin and biglycan were injected at 5 mg/kg body weight, every other day until day 20 post-injection. Tumor sizes were assessed throughout the experiment by caliper measurements of length (L) and width (W), and tumor volume (V) was calculated using the formula: V (in mm^3) = 0.5 x L x W^2. When the largest tumor reached 2000 mm^3 in size, mice were sacrificed by CO_2 inhalation and tumors were surgically dissected and divided into two halves. One half of the sample was flash frozen in liquid N_2 and stored at -80°C for further biochemical analysis. The other half was kept in 10% buffered formalin for 24 h and processed by a sequential incubation in 15% and 30% sucrose in PBS for 24 h each. The samples were then embedded in OCT (Sakura Finetek, CA, USA) medium and stored at -80°C; 8-10 µm thick sections were generated utilizing a cryostat (Leica CM1860) from the frozen tumor tissue, mounted on superfrost plus (Fisherbrand, 22-037-246) glass slides, dried via vacuum for 18 h and stored at -80ºC until needed or processed for immunofluorescence analysis.

Preparation of 3D Collagen Type I Matrix and Thoracic Duct Isolation from Mice

We used a mixture of rat-tail collagen type I (Corning, 354236); media 199 10X phenol red free (ThermoFisher Scientific); 140 mM $NaHCO_3$ (filter sterilized); 1 M NaOH (dissolved in autoclaved water) and ultrapure sterile water. For 10ml mixture, we used 4.33 ml of collagen type I, 1.53 ml of 10X media 199, 4.12 ml of 140 mM $NaHCO_3$, 0.45 ml of sterile water and 18µl of 1M NaOH. At the neutral pH, pink buffered collagen mixture was added to the desired culture plate to cover the bottom and allowed to polymerize at 37°C. Following anesthetization with isoflurane, 4% Evans blue, a vital dye that is absorbed via the lymph (10), was injected into both hind footpads of the C57BL/6 wild type mice and blue stained dye was allowed to travel through the lymphatic system and stain thoracic duct for 6-8min. After sacrificing the mice with CO_2 inhalation, the blue-stained thoracic duct adjacent to the aorta was carefully dissected out from the opened chested cavity as shown in Fig S2. After trimming most of the fat from the isolated thoracic duct, it was chopped into small pieces and each small piece was embedded in the previously prepared culture plate with type I collagen. Each sectioned lymphatic ring was sandwiched with another layer of top collagen mixture described above for 30 min, and finally endothelial cell media (Cell Biologics, M1168) was added on top of it to facilitate lymphatic vessel sprouting at 37°C in 5% CO_2. We were successfully able to grow at least 10-20 rings of ~1 mm in width from the thoracic duct of each C57BL/6 mice. Either 400 nM of decorin or biglycan was added for 3 consecutive days after day 3 of LR explant when sprouting begins (Fig. S3). After Day 6 –of growing LRs on the collagen in absence or presence 3 days of chronic decorin/biglycan, bright field images were captured at 4X in Leica DM IL LED inverted microscope for analysis with ImageJ software (https://imagej.net/Fiji/) and further processed for immunoblotting and immunostaining.

Measuring Radial Distance of the Sprouts

Next, each captured image of the representative rings after Day 6, was analyzed using ImageJ software. We typically observed sprouting after Day 3 around the LRs. From Day 5, dense vessel sprouting could be observed from each lymphatic ring. Sprouting is mostly branched from the sides of the lymphatic ring. So, here we propose a method through ImageJ where one can precisely measure the distance travelled by the sprouts from the end of the thoracic duct. After day 6, phase contrast images of the live explants were acquired, and using the subtract background function in ImageJ, background was removed from each image using the rolling ball radius of 700 pixels. This step reduces noise and improves contrast. Next, the sprouts were exclusively highlighted in red using the adjust threshold function, eliminating the lymphatic ring and any empty spaces. Finally, using the set scale function, the accurate pixel/micron ratio was entered based on the resolution settings of the microscope and magnification of the objective lens (i.e. 0.645 µm/pixel), and check the global setting option. Using the circle option on the ImageJ toolbar, a circle was drawn around the highlighted sprouts and another around the lymphatic ring (Fig. S4). Using the measure function, the radii of each circle were determined, and the radius of the larger circle was subtracted from that of the smaller one to calculate the radial distance of the sprouts.

RNAseq and Bioinformatics Analyses

We performed high-throughput deep RNAseq (Genewiz, NJ) from the orthotopic mammary tumor allografts of 14 mice (RNAseq data available at www.iozzolab.com). We validate RNA integrity through capillary electrophoresis and mRNA was enriched and sequenced utilizing the Illumina® HiSeq® system configured at 2x150 bp. Sequence reads were trimmed to remove possible adapter sequences and poor-quality nucleotides using Trimmomatic v.0.36(11) and mapped to the Mus musculus GRCm38 reference genome (ENSEMBL) using STAR aligner v.2.5.2b(12). Unique gene hits were calculated via Counts from the Subread v.1.5.2. At the protein level, we used STRING v11 database to get score for protein/protein interactions networks (13). We queried datasets from three different breast cancer cohorts (14-16) where expression and grade information were curated using ShinyGEO (17). We used KMplotter (18, 19) from GEO & EGA repositories to determine the role of high and low DCN expression and survival in breast carcinoma patients.

Imaging Studies

For immunostaining, antibodies were obtained from the following sources: anti-6x-His (1:200, ab18184), β-catenin (1:100, ab16051), CD31 (1:100, ab222783), Podoplanin (1:100, ab10288), Beclin1 (1:200, ab62557) from Abcam (Cambridge, MA, USA). Lyve1 (1:50, 14-0443-82) and LC3 (1:100, L7543) were purchased from ThermoFisher Scientific (Waltham, MA, USA) and Sigma Aldrich (St. Louis, MO, USA).

Secondary antibodies like goat anti-mouse Alexa Fluor™ 488 (A-11001), goat anti-rat Alexa Fluor™ 594 (A-11007), goat anti-mouse Alexa Fluor™ 594 (A-11004) and donkey anti-rabbit Alexa Fluor™ 488 (A-21206) were purchased from ThermoFisher Scientific and used at 1:400 dilution. Freshly prepared or frozen tumor sections mounted on glass slides were blocked with 1% BSA in PBS for 1 h followed by incubation with respective primary antibody for 1 h at room temperature. Slides were washed three times with PBS after the primary antibody incubation to remove any remaining stain and further probed with respective secondary antibody at 1:400 dilution for 1 h in the dark. To remove the excess stain, slides were washed again with PBS and allowed to dry for 1 min. We avoided over drying the slides anytime during the process. VECTASHIELD antifade mounting medium with DAPI (Vector Laboratories, H-1500) was added and a clean coverslip was placed on top of the tissue section and finally sealed the four corners with sealer before visualizing in a Leica DM5500 B fluorescence microscope. 3D collagen embedded LRs treated with and without 3 days of chronic decorin and differentially treated mouse LECs were fixed with 4% paraformaldehyde (PFA) for 30 min followed by permeabilization with 0.1% Triton-X100 at room temperature. Mouse LECs were grown on a glass coverslip in a 12 well culture plate at 37ºC at 5% CO_2. After fixation, 1% BSA in PBS was used as blocking agent for 1 h and primary antibodies diluted in blocking solution were incubated for 2 h in room temperature for mouse LECs and overnight for LRs. After washing the primary antibody with PBS three times with gentle shaking, respective secondary antibodies were added and incubated for another 2 h. To remove the excess unbound secondary, samples were again washed three times with PBS, stained with DAPI and finally visualized in either Leica DM5500 B fluorescence or Nikon A1R inverted confocal microscope.

Immunoblotting and Inhibitors

For Western blotting, antibodies were procured from the following sources: β-catenin (1:1000, ab16051), CD31 (1:1000, ab222783), podoplanin (1:500, ab10288) and beclin1 (1:2000, ab62557) from Abcam. Has2 (sc-514737) was purchased from Santa Cruz Biotechnology (1:500, Santa Cruz, CA, USA). Lyve1 (1:500, #67538), GAPDH (1:4000, #2118), Phospho-Akt (Ser473) (1:500, #9271) and Akt antibody (1:1000, #9272) were obtained from Cell Signaling Technology (Beverly, MA, USA). Human VEGFR3/Flt-4 antibody (1:200, 20712-1-AP) was obtained from Proteintech (Rosemont, IL, USA) Horse Radish Peroxidase (HRP) conjugated secondary antibodies like goat anti-rabbit (Millipore, AP307P, 1:3000), goat anti-mouse (Promega, W4021, dilution 1:3000) were used for this study. Similarly, weighted samples of the flash frozen tumors were crushed with liquid nitrogen in a pestle to lyophilize and tumor lysates were prepared after lysing the lyophilized material in RIPA buffer: 50 mM Tris-Cl; pH 7.5, 150 mM NaCl, 1 mM EGTA, 1 mM EDTA, 0.5% deoxycholate, 0.5% SDS, 1% Triton-X 100, 1 mM orthovanadate, 1 mM PMSF, plus protease inhibitor cocktail, (ThermoFisher, #A32961). To prepare the LR lysates from *ex vivo* 3D model, three sprouted LRs with or without three-day chronic decorin treatment were pooled with RIPA lysis buffer to enhance the protein yield and lysed with sonication on ice. Mouse and human LECs were cultured in 12-well plates at a density of 1 x 10^5 cells/ml and at around 70% confluency, all the experiments were done as indicated in the study. LECs were lysed in RIPA after scrapping and all the lysates including tumor and LR lysates were mixed with 5X SDS sample buffer [250 mM Tris-HCl, pH 6.8, 10% (wt/vol) SDS, 40% (vol/vol) glycerol, 5 % β-mercaptoethanol] and boiled at 100°C for 8-10 min. Protein concentration was measured by Pierce™ BCA Protein Assay Kit and equal amounts of protein after lysis were loaded on SDS-PAGE. Proteins were separated on 10 % or 14% SDS-PAGE and transferred to nitrocellulose membranes (#10600002, GE Healthcare Biosciences). The membranes were blocked with 1% BSA in TBS-Tween 20 (TBST) for 1 h and then incubated with respective primary antibodies diluted in blocking solution for overnight. After washing in TBST, membranes were probed with secondary antibodies for 1 h at room temperature. Finally, membranes were again washed three times with TBST and submerged in SuperSignal West Pico chemiluminescent substrate for 2 min before visualizing through ImageQuant LAS 4000 chemiluminescent Image analyzer (GE Healthcare). Blots were quantified by densitometric measurement of each protein normalized to the Gapdh loading control through Image J.

We used a variety of inhibitors including two specific mTOR inhibitors, Torin 1 (20, 21) and INK128 (22). Torin 1 (S2827), INK128 (S2811), SAR131675 (S2842) and Anlotinib (S8726) were purchased from Selleckchem (Houston, TX). Bafilomycin A1 was purchased from InvivoGen (tlrl-baf1, San Diego, CA) (23, 24).

Quantitative PCR (qPCR) Analysis

Total mRNA was extracted from a pool of 3 sprouted LRs or breast tumor allografts treated with or without decorin by GenElute™ Single Cell RNA Purification Kit (Sigma-Aldrich, RNB300) as per manufacturer's protocol. DNase I (Invitrogen) treatment was performed to remove any DNA contaminants from the isolated total mRNA. 0.5-1 µg of RNA was used for complementary DNA synthesis using SuperScript cDNA Synthesis Kit (ThermoFischer Scientific, 11750150) and utilized for real time PCR using different primer sets listed in Table S1. Quality of RNA was verified by running 2% agarose gel, and qPCR was performed on the Step One Real-Time PCR system (Applied Biosystems, Foster City, CA, USA) using SYBR Green PCR Master Mix II (Agilent Technologies). Amplicons representing target genes and the endogenous housekeeping gene, β-actin, were amplified in at least triplicate, independent reactions. Fold change determinations were made using the Comparative Ct method for expression analysis and fold changes were calculated using the double ΔCt method ($2^{-\Delta\Delta CT}$) ± SEM. Relative expression level of the target genes was normalized with untreated control as a reference sample keeping actin as the endogenous control.

Solid-phase Binding Assays

Direct binding of decorin protein core to the soluble Fc tagged VEGFR3 (sVEGFR3-Fc, R&D systems, 349-F4), was performed using solid-phase binding assay. ELISAs were performed according to a standard protocol as shown previously (25, 26). Decorin or sVEGFR3-Fc (100 ng/well) was allowed to adhere to the 96 well plate overnight at RT in the presence of carbonate buffer, pH 9.6. Plates were washed with PBS, incubated for 2 h with serial dilutions of decorin protein core or sVEGFR3. In the quantitative competition experiment, decorin protein core was kept at constant concentration (50 nM) and incubated with increasing concentrations of VEGFC. After incubation, plates were extensively washed with PBS, blocked with 1% BSA/ in PBS, and incubated for 1 h with an antibody raised against decorin (27) or VEGFR3 (R&D systems). HRP-conjugated secondary antibody was incubated for 1 h and the immune complexes were revealed using SIGMA-FAST ™ O-phenylenediamine dihydrochloride (P9187). Absorbance at 490 nm was measured in a Victor3TM (PerkinElmer Life Sciences).

Phospho-VEGFR3 Sandwich ELISA

Phosphorylation of VEGFR3 was estimated by sandwich ELISA as shown in previous report with minor modifications (28). Human dermal LECs were plated on ~~a~~ 12 well plates at a density of 1 x 10^5 cell/ml and at 60-70% confluency, LECs were serum starved for 24 h at 37°C. According to the experimental need, serum starved human LECs were pre-treated with 5µM SAR131675 or Anlotinib for 30 min, before VEGF-C or decorin stimulation for 20 minutes. The media was then aspirated, and the cells were washed once with cold PBS before being lysed with 150 µl lysis buffer: 1% NP-40. 20 mM Tris [pH 8.0], 137 mM NaCl, 10% glycerol, 2 mM EDTA, 1 mM activated sodium orthovanadate, and 10% protease inhibitors. Then lysates were utilized exactly according to the instructions in the Human Phospho- VEGFR3/Flt-4 DuoSet IC ELISA Kit (R&D systems, DYC2724-5). Ninety-six well microplate was first coated with primary human phospho-VEGFR3 capture antibody overnight at room temperature, then washed and blocked at room temperature for 1 h with blocking buffer. After washing the blocking buffer, differentially treated cell lysates with a positive control (provided in the kit) were added to the microplate for 2 h at room temperature. After washing the microplate well, secondary anti-PY-HRP antibody was added for another 2 h in the dark followed by washing. Subsequently, substrate solution was added to each well, incubated for 15 min in the dark and the reaction was stopped by adding stop solution. Finally, after gentle tapping and mixing the plate in a shaker, optical density was measured using a microplate reader set at 450 nm. Wavelength correction was made by subtracting the optical imperfections of reading measured at 540 nm.

Statistical Analyses

All statistical analyses were performed using Prism 9 (GraphPad Software, Inc., San Diego, CA), and details can be found in the respective figure legends. We used when appropriate one-way analysis of variance (ANOVA) or Student's *t*-test. *P* values smaller than 0.05 were considered statistically significant.

Supplementary Table and Figures

Supplementary Table 1. List of primers used in qPCR

Gene	Forward primer (5' – 3')	Reverse primer (3' – 5')
Actb	ACCTTCTACAATGAGCTGCG	CTGGATGGCTACGTACATGG
Becn1	TTTTCTGGACTGTGTGCAGC	GCTTTTGTCCACTGCTCCTC
Cxcl12	CAGCTCTCCTACCCTGTATCT	TGCCACAGGACAAACAGTAG
Fgf7	AAGACTGTTCTGTCGCACC	CACTTTCCACCCCTTTGATTG
Fgf9	GGAACCAGGAAAGACCACAG	TTTTCTGATCCATACAGCTCCC
Map1lc3b	TTCTTCCTCCTGGTGAATGG	GTGGGTGCCTACGTTCTCAT
Lyve1	CAGCATTCAAGAACGAAGCAG	GCCTTCACATACCTTTTCACG
Mmp3	GATGAACGATGGACAGAGGATG	AAACGGGACAAGTCTGTGG
Pdpn	GTGACCCCAGGTACAGGAGA	GCTGAGGTGGACAGTTCCTC
Prox1	CTGCTAGTGGACCTGATCTTTAC	CCTGGTCAGCTGCTTTAAGATA

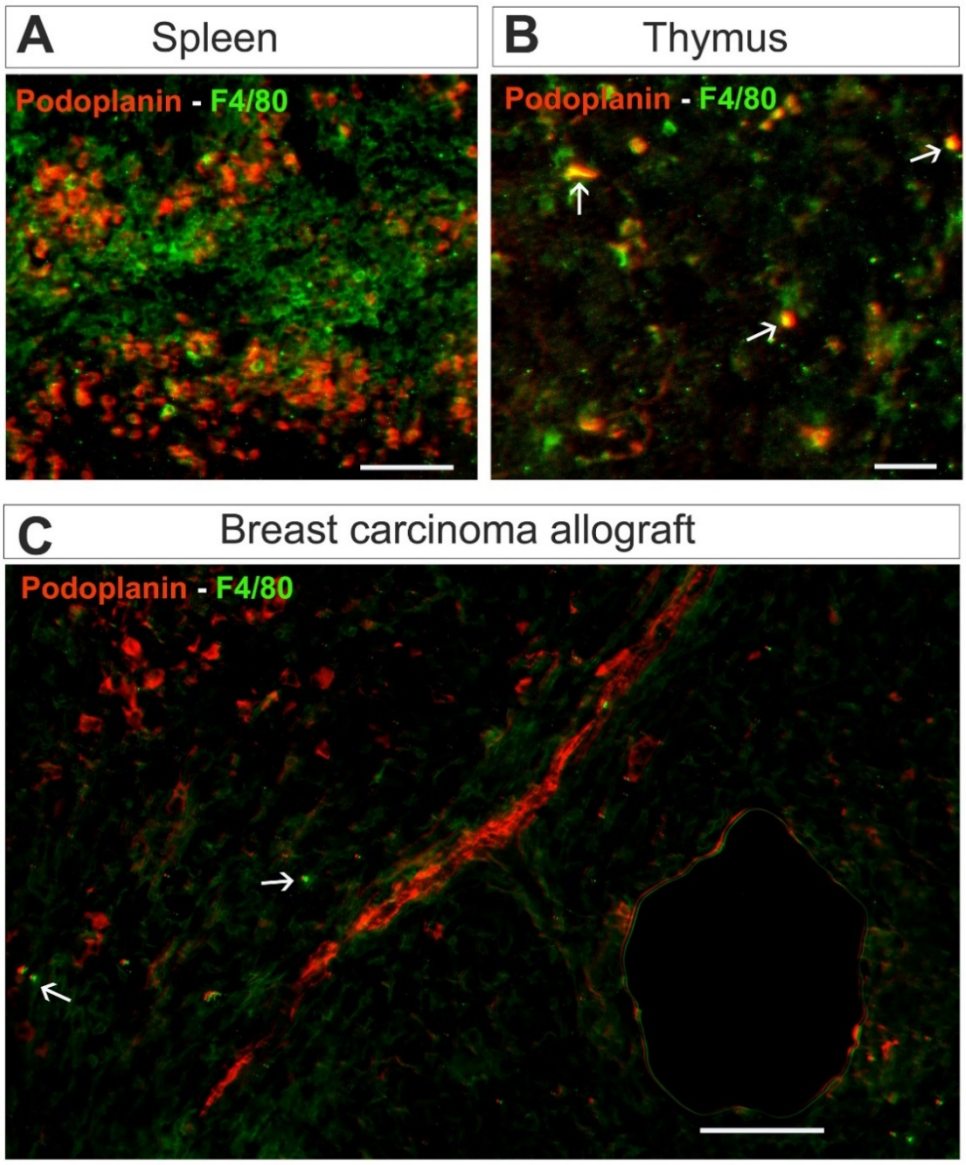

Fig. S1. Representative immunofluorescence analysis of frozen sections from spleen (A), thymus (B) and breast carcinoma allografts (C), immunolabeled for podoplanin (red) and F4/80 (green). In the spleen, two different populations of cells are clearly visible unlike the thymus which exhibits greater colocalization with distinct orange puncta. White arrows indicate the orange puncta with greater colocalization. In breast carcinoma allografts, we found very few macrophages (white arrows) which do not colocalize with intense staining of lymphatic marker podoplanin. Images were captured using a Nikon Eclipse Ts2 fluorescence microscope and utilizing 12-14 z stacks. Bars ~250 μm.

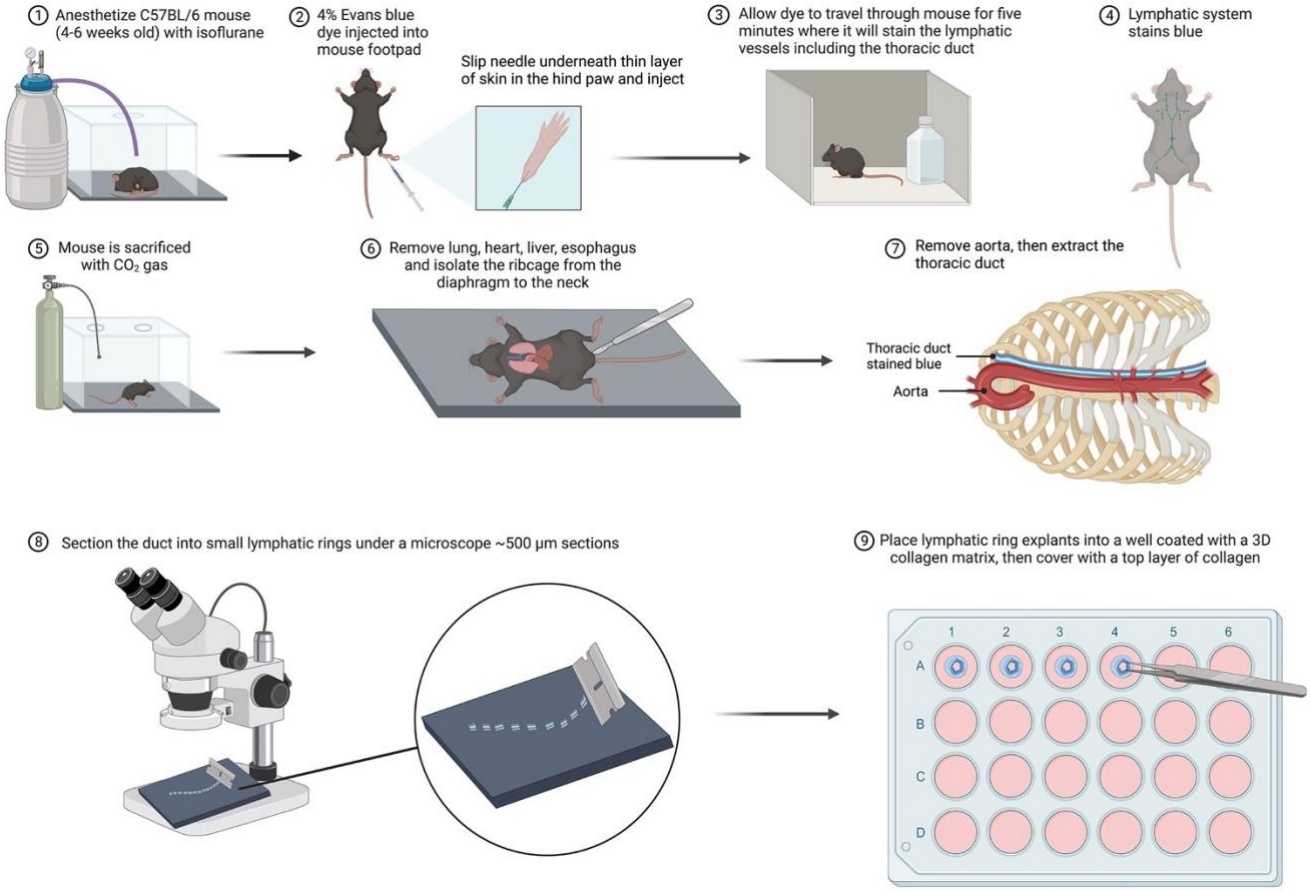

Fig. S2. Schematic representation of the generation of lymphatic ring explants from C57BL/6 mice and their growth in an *ex vivo* 3D matrix composed rat tail collagen type I. Each step starting from anesthetizing the mice, to removing the thoracic duct from chest cavity and growing a piece of sectioned duct on 3D collagen matrix are clearly shown here. The image is self-explanatory and was created using *Biorender.com*.

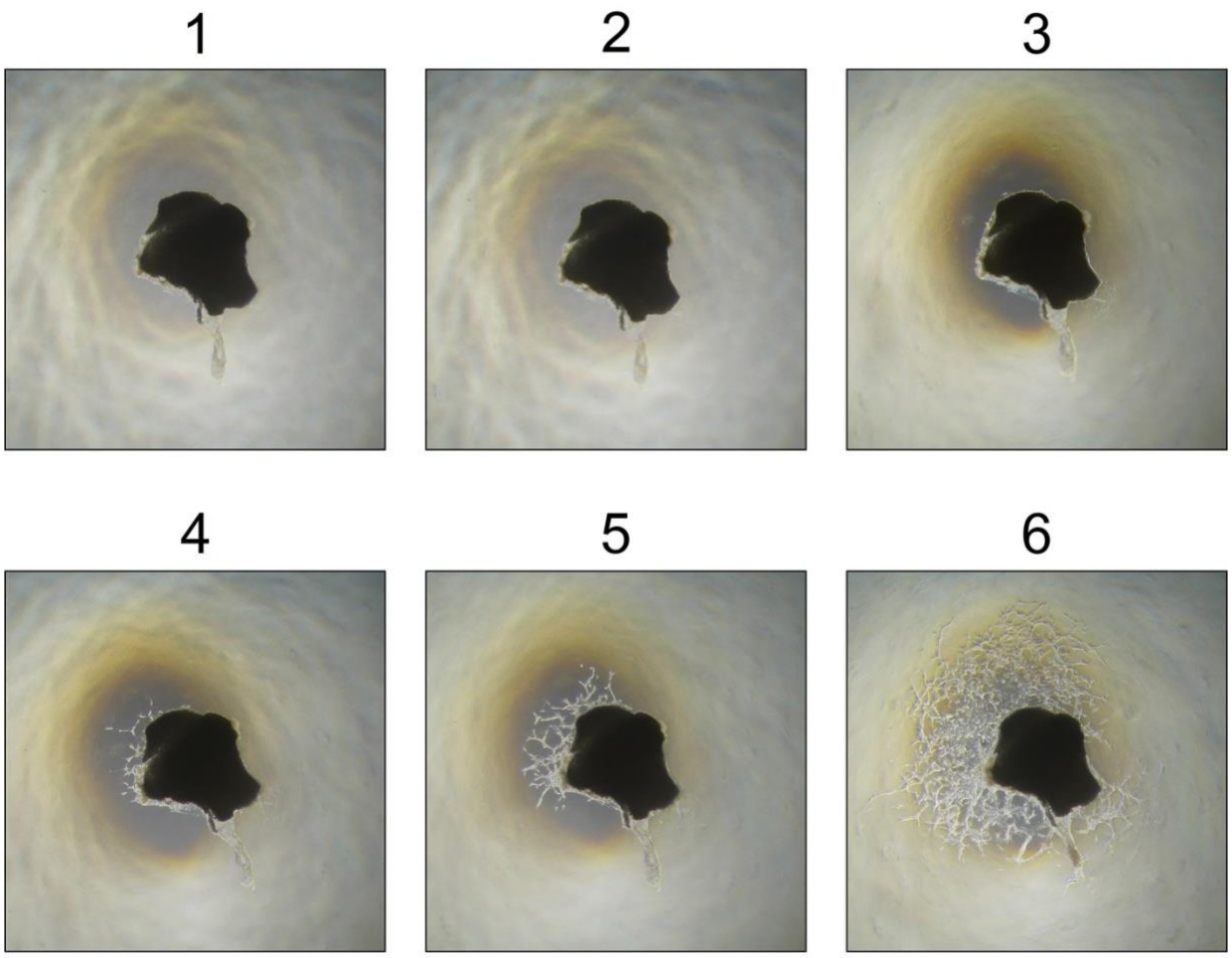

Fig. S3. Day wise progression of lymphatic ring sprouting in the *ex vivo* assay. Bright field images of a representative lymphatic ring were taken at every day for six days at 4X magnification in an inverted Leica bright field microscope. Day 5 onwards, outgrowths from the LR migrate rapidly far from the LR and becomes so concentrated by the end of Day 6. Raw images after day 6 were taken and further analyzed for axial radial distance measurement.

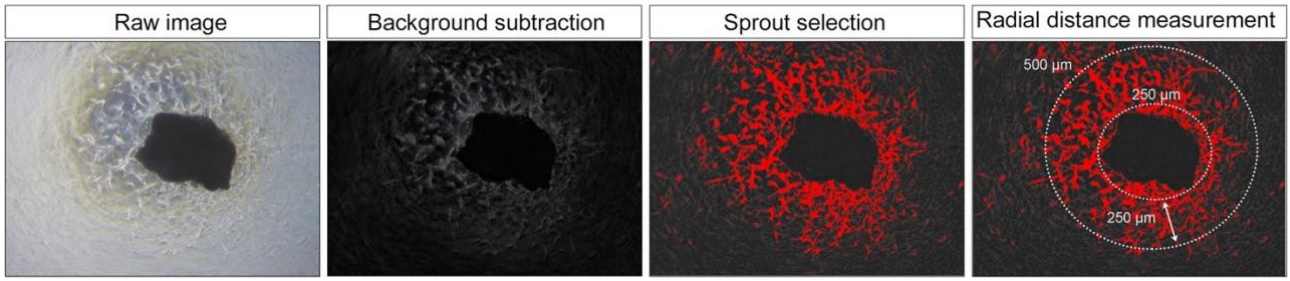

Fig. S4. Axial radial distance measurement of the lymphatic ring sprouting. Each step of the radial distance calculation was performed using ImageJ from the raw images, after subtracting the background and selecting only the sprouts in red. Distance travelled by the sprouts was finally measured after subtracting the radius of the two circles as shown here.

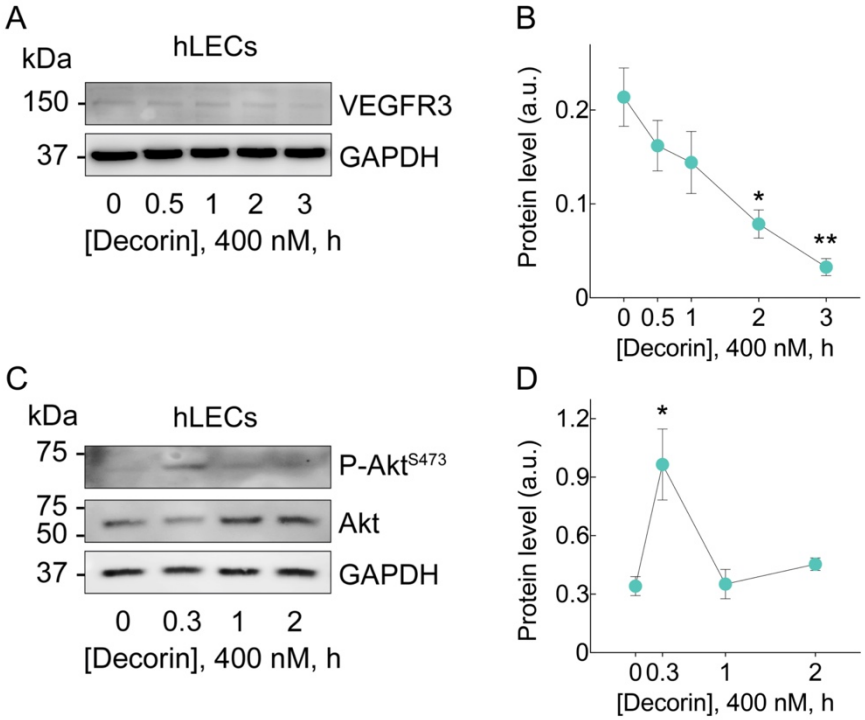

Fig. S5. Decorin time course experiment on primary human LECs. (A) Representative immunoblotting for VEGFR3 and GAPDH. Lysates were separated on 9% SDS-PAGE as indicated above and probed for VEGFR3, and GAPDH. (B) Relative quantification of VEGFR3 expression at the indicated time points normalized on GAPDH. One way ANOVA; **P*<0.05; ***P*<0.01. (C) Representative Immunoblotting for P-Akt at Ser^{473}, total Akt and GAPDH. The cells were rendered quiescent by serum starvation for 18 h, and then treated with soluble decorin at the indicated time intervals. (D) Relative amounts of P-Akt levels normalized on total Akt. One way ANOVA; **P*<0.05.

References

1. A.Ewens, E.Mihich, M.J.Ehrke, Distant metastasis from subcutaneously grown E0771 medullary breast adenocarcinoma. *AntiCancer Res.* **25**:3905-3915 (2005).
2. A.Casey, W.R.Jr.Laster, Ross G.L, Sustained enhanced growth of carcinoma EO771 in C57 black mice. *Proc. Soc. Exp. Biol Med.* **77**:358-362 (1951).
3. A.Ewens *et al.*, Doxorubicin plus interleukin-2 chemoimmunotherapy against breast cancer in mice. *Cancer Res.* **66**:5419-5426 (2006).
4. D.Dong *et al.*, A critical role for GRP78/BiP in the tumor microenvironment for neovascularization during tumor growth and metastasis. *Cancer Res.* **71**:2848-2857 (2011).
5. Z.Zou *et al.*, Inhibition of the HER2 pathway by n-3 polyunsaturated fatty acids prevents breast cancer in fat-1 transgenic mice. *J. Lipid Res.* **54**:3453-3463 (2013).
6. C.N.Johnstone *et al.*, Functional and molecular characterisation of EO771.LMB tumours, a new C57BL/6-mouse-derived model of spontaneously metastatic mammary cancer. *Dis. Model. Mech.* **8**:237-251 (2015).
7. T.Hiraga, T.Ninomiya, Establishment and characterization of a C57BL/6 mouse model of bone metastasis of breast cancer. *J. Bone Miner. Metab* **37**:235-242 (2019).
8. I.X.Chen *et al.*, Blocking CXCR4 alleviates desmoplasia, increases T-lymphocyte infiltration, and improves immunotherapy in metastatic breast cancer. *Proc. Natl. Acad. Sci. U. S. A* **116**:4558-4566 (2019).
9. K.G.Danielson *et al.*, Targeted disruption of decorin leads to abnormal collagen fibril morphology and skin fragility. *J. Cell Biol.* **136**:729-743 (1997).
10. M.I.Harrell, B.M.Iritani, A.Ruddell, Lymph node mapping in the mouse. *J. Immunol. Methods* **332**:170-174 (2008).
11. A.M.Bolger, M.Lohse, B.Usadel, Trimmomatic: a flexible trimmer for Illumina sequence data. *Bioinformatics.* **30**:2114-2120 (2014).
12. A.Dobin *et al.*, STAR: ultrafast universal RNA-seq aligner. *Bioinformatics.* **29**:15-21 (2013).
13. D.Szklarczyk *et al.*, STRING v11: protein-protein association networks with increased coverage, supporting functional discovery in genome-wide experimental datasets. *Nucleic Acids Res.* **47**:D607-D613 (2019).
14. C.Desmedt *et al.*, Strong time dependence of the 76-gene prognostic signature for node-negative breast cancer patients in the TRANSBIG multicenter independent validation series. *Clin. Cancer Res.* **13**:3207-3214 (2007).
15. G.Jönsson *et al.*, The retinoblastoma gene undergoes rearrangements in BRCA1-deficient basal-like breast cancer. *Cancer Res.* **72**:4028-4036 (2012).
16. M.Schmidt *et al.*, The humoral immune system has a key prognostic impact in node-negative breast cancer. *Cancer Res.* **68**:5405-5413 (2008).
17. J.Dumas, M.A.Gargano, G.M.Dancik, shinyGEO: a web-based application for analyzing gene expression omnibus datasets. *Bioinformatics.* **32**:3679-3681 (2016).
18. B.Győrffy *et al.*, An online survival analysis tool to rapidly assess the effect of 22,277 genes on breast cancer prognosis using microarray data of 1,809 patients. *Breast Cancer Res. Treat.* **123**:725-731 (2010).
19. Z.Mihály *et al.*, A meta-analysis of gene expression-based biomarkers predicting outcome after tamoxifen treatment in breast cancer. *Breast Cancer Res. Treat.* **140**:219-232 (2013).
20. C.C.Thoreen *et al.*, An ATP-competitive mammalian target of rapamycin inhibitor reveals rapamycin-resistant functions of mTORC1. *J. Biol. Chem.* **284**:8023-8032 (2009).
21. Q.Liu, C.Thoreen, J.Wang, D.Sabatini, N.S.Gray, mTOR mediated anti-cancer drug discovery. *Drug Discov. Today Ther. Strateg.* **6**:47-55 (2009).
22. A.C.Hsieh *et al.*, The translational landscape of mTOR signalling steers cancer initiation and metastasis. *Nature* **485**:55-61 (2012).
23. E.J.Bowman, A.Siebers, K.Altendorf, Bafilomycins: a class of inhibitors of membrane ATPases from microorganisms, animal cells, and plant cells. *Proc. Natl. Acad. Sci. U. S. A* **85**:7972-7976 (1988).
24. T.Yoshimori, A.Yamamoto, Y.Moriyama, M.Futai, Y.Tashiro, Bafilomycin A1, a specific inhibitor of vacuolar-type H(+)-ATPase, inhibits acidification and protein degradation in lysosomes of cultured cells. *J. Biol Chem.* **266**:17707-17712 (1991).

25. T.Neill *et al.*, EphA2 is a functional receptor for the growth factor progranulin. *J. Cell Biol* **215**:687-703 (2016).
26. A.Goyal *et al.*, Endorepellin, the angiostatic module of perlecan, interacts with both the a2b1 integrin and vascular endothelial growth factor receptor 2 (VEGFR2). *J. Biol. Chem.* **286**:25947-25962 (2011).
27. S.Goldoni *et al.*, Biologically active decorin is a monomer in solution. *J. Biol. Chem.* **279**:6606-6612 (2004).
28. H.M.Bui *et al.*, Proteolytic activation defines distinct lymphangiogenic mechanisms for VEGFC and VEGFD. *J. Clin. Invest* **126**:2167-2180 (2016).